Proceedings of the 1997 IEEE
International Conference on Robotics and Automation
Albuquerque, New Mexico - April 1997

Visual Servoing of Nonholonomic Cart

Koichi Hashimoto and Toshiro Noritsugu

Department of Systems Engineering
Okayama University
3-1-1 Tsushima-naka, Okayama 700 JAPAN

Abstract— **This paper presents a visual feedback control scheme for a nonholonomic cart without capabilities for dead reckoning. A camera is mounted on the cart and it observes cues attached on the environment. The dynamics of the cart are transformed into a coordinate system in the image plane. An image-based controller which linearizes the dynamics is proposed. Since the positions of the cues in the image plane are controlled directly, possibility of missing cues is reduced considerably. Simulations are carried out to evaluate the validity of the proposed scheme. Experiments on a radio controlled car with a CCD camera are also given.**

I. Introduction

A typical approach for autonomous mobile robot navigation is dead reckoning, which is based on the map of the work space as well as the position and orientation estimates produced by using wheel rotation information. However, the cart considered in this paper is a plastic model and it does not have dead reckoning capability. Thus, a pure external sensor feedback control scheme have to be implemented. In this paper, we use a camera as an external sensor.

An interesting problem of controlling a cart is the nonholonomic constraints, which does not decrease the degree of freedom of the system. Control and path planning of systems with nonholonomic constraints are areas of active research. As pointed out in [1], the problem has been addressed from two points of view, i.e., (1) open-loop strategies that seek to find a bounded sequence of control inputs to steer the cart from any initial position to any other arbitrary configuration [2], [3], [4] and (2) closed-loop strategies consist of designing feedback loops stabilizing the cart about an arbitrary point in the state space [5], [1], [6], [7], [8]. Some interesting comparisons of these approaches can be found in [9] and a summary of algorithms is given in [10].

This paper proposes a closed-loop control scheme based on visual feedback. The control law is solely based on the information obtained by the camera mounted on the cart. The camera observes visual cues attached on the environment. Our scheme is different from the vision-based mobile robot developed by Baumgartner and Skaar [11] because their scheme is based on the path generated by the open-loop controller. Previous Cartesian space control laws for nonholonomic cart are not suitable for driving our vision-based cart because the generated steering angle commands tend to be large enough to loose the visual cues out of sight. Thus we propose an image-based visual servoing controller. The controller is a piecewise smooth exponentially stabilizing controller in the image coordinates, which is an extension of the controller proposed by Canudas de Wit and Sørdalen [1]. It generates driving inputs for the cart so as to the image of the cues converges to the goal position along a path in the image plane. Therefore, possibility of missing the cues out of sight reduces considerably. The term "image-based" is used in contrast to "position-based" which reproduces the position and orientation information from the visual information obtained by the camera [12].

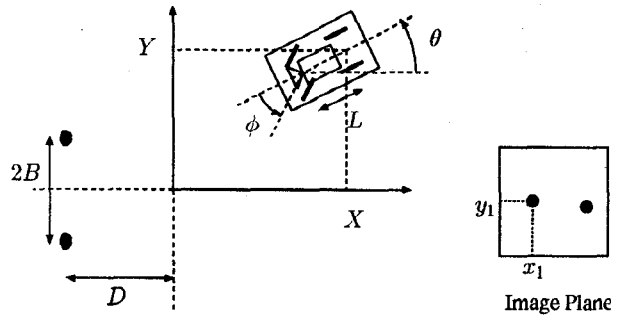

Fig. 1. Kinematic Model of Cart

Validity of the proposed method is evaluated by simulations with four wheel cart. A comparison with position-based controller [1] is also made. Experiments on a radio controlled cart with a CCD camera attached on the roof are conducted. The results show validity of the proposed algorithm.

II. Kinematic Model

Figure 1 shows a schematic diagram of a cart with four wheels. We assume that the cart is driven by rear wheels and the wheels do not slip. The front and rear pairs of wheels are considered as single wheels at the midpoints of the axles. Let X, Y, θ denote the position and orientation of the cart, where (X, Y) is the position of the midpoint of the rear axle and θ is the angle

between the X axis and the line connecting the front and rear midpoints. The inputs to the car are ϕ, the steering angle with respect to the cart body, and v, the velocity of the rear wheel. Then the kinematic model is given by [13]

$$\begin{aligned} \dot{X} &= v\cos\theta \\ \dot{Y} &= v\sin\theta \\ \dot{\theta} &= \omega = \frac{v}{L}\tan\phi \end{aligned} \tag{1}$$

where L is the length between front and rear wheels (wheel base). This system has constrains

$$\begin{aligned} \sin(\theta+\phi)\dot{X} - \cos(\theta+\phi)\dot{Y} - L\cos\phi\dot{\theta} &= 0 \\ \sin\theta\dot{X} - \cos\theta\dot{Y} &= 0 \end{aligned} \tag{2}$$

due to the assumption of no slippage (the left hand sides of these equations are the velocities of rear wheels perpendicular to the way they are pointing). Consider $p = [X\ Y\ \theta]^T$ as the state vector and $u = [v\ \phi]^T$ as the input vector, then we have

$$\dot{p} = Gg(u) \tag{3}$$

where

$$\begin{aligned} G &= \begin{bmatrix} \cos\theta & 0 \\ \sin\theta & 0 \\ 0 & 1 \end{bmatrix}, \\ g(u) &= \begin{bmatrix} v \\ \omega \end{bmatrix} = \begin{bmatrix} v \\ \frac{v}{L}\tan\phi \end{bmatrix}. \end{aligned} \tag{4}$$

Equation (3) is called the kinematic model of the cart.

III. Visual Information

As shown in Figure 1, a camera is mounted on the cart. The camera's optical axis is aligned with the line connecting the front and rear midpoints of the axis. Suppose that there are two visual cues on the wall with distance D from the origin. Let the distance between the two cues be $2B$ and the relative height of the cues with respect to the camera be h. Assume that the camera characteristics are modeled by ideal perspective projection with f being the focal length. Then the map between the positions of the cues in the image plane denoted by $\xi = [x_1\ y_1\ x_2\ y_2]^T$ and the position/orientation of the cart p becomes

$$\xi = \iota(p), \tag{5}$$

where

$$\begin{aligned} \iota(p) &= [-f\tfrac{m_3}{m_1}\quad f\tfrac{h}{m_1}\quad -f\tfrac{m_4}{m_2}\quad f\tfrac{h}{m_2}]^T \\ m_1 &= (X+D)\cos\theta + (Y+B)\sin\theta \\ m_2 &= (X+D)\cos\theta + (Y-B)\sin\theta \\ m_3 &= (Y+B)\cos\theta - (X+D)\sin\theta \\ m_4 &= (Y-B)\cos\theta - (X+D)\sin\theta. \end{aligned} \tag{6}$$

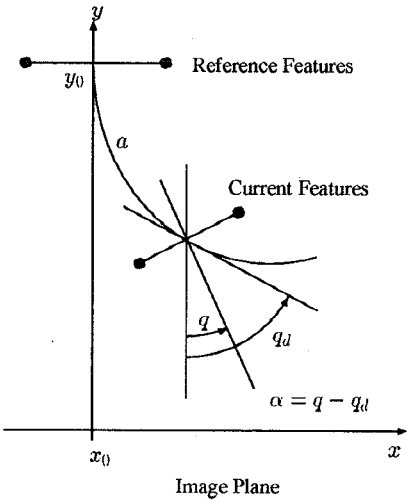

Fig. 2. Coordinate Transformation

IV. Coordinate Transformation

The image coordinates of the features when the cart is at the goal position are called the reference features. Let p_d be the goal position, then $\xi_d = [x_{1d}\ y_{1d}\ x_{2d}\ y_{2d}]^T = \iota(p_d)$ is the reference feature vector. In this paper, we assume that $p_d = 0$ and we have

$$\xi_d = [-f\tfrac{B}{D}\quad f\tfrac{h}{D}\quad f\tfrac{B}{D}\quad f\tfrac{h}{D}]^T. \tag{7}$$

Figure 2 shows reference and current features in the image plane. Let the midpoint of the goal features be

$$(x_0,\ y_0) = (\frac{x_{1d}+x_{2d}}{2},\ \frac{y_{1d}+y_{2d}}{2}) \tag{8}$$

and consider a family of circle

$$\mathcal{P} = \{(x,y) : (x - x_0 - r)^2 + (y - y_0) = r^2\} \tag{9}$$

in the image plane. These circles pass through the midpoint of the goal features $(x_0,\ y_0)$ and the midpoint of the current feature

$$(x_c,\ y_c) = (\frac{x_1+x_2}{2},\ \frac{y_1+y_2}{2}). \tag{10}$$

Also they are centered on the $y = y_0$ line with $\frac{\partial x}{\partial y} = 0$ at $y = y_0$. Let a denote the arc length between the two midpoints; q_d denote the angle of the tangent of $\mathcal{P}$ at (x_c, y_c); and q denote the angle of the normal of the line segment between the current features. Note that these angles are with respect to the y axis the image plane. Then we have

$$\begin{aligned} q &= \arctan\frac{y_{21}}{x_{21}} \\ q_d &= 2\arctan\frac{x_{c0}}{y_{c0}} \\ a &= rq_d = \frac{x_{c0}^2 + y_{c0}^2}{x_{c0}}\arctan\frac{x_{c0}}{y_{c0}} \end{aligned} \tag{11}$$

where $x_{21} = x_2 - x_1$, $y_{21} = y_2 - y_1$, $x_{c0} = x_c - x_0$ and $y_{c0} = -y_c + y_0$. Define the controlled variable as

$$z = \begin{bmatrix} a \\ \alpha \end{bmatrix}^T, \tag{12}$$

where $\alpha = q - q_d$. Then, controlling the cart so as to reduce a and α to zero yields a control input which guarantees the visual cues to lie inside the view area of the camera. This is an important feature of the image-based visual servoing.

V. Model for Visual Servoing

Note that z is a smooth function of ξ. Also ξ is a smooth function of p. Differentiation of z gives.

$$\dot{z} = \frac{d}{dt}\begin{bmatrix} a \\ \alpha \end{bmatrix} = \frac{\partial z}{\partial \xi}\frac{\partial \xi}{\partial p} G q(u) = JFGq(u) \tag{13}$$

where

$$\begin{aligned} J &= \begin{bmatrix} l_1 & l_2 & l_1 & l_2 \\ l_3 + l_5 & -l_4 + l_6 & -l_3 + l_5 & l_4 + l_6 \end{bmatrix}, \\ l_1 &= \frac{1}{2}\left(\frac{(x_{c0}^2 - y_{c0}^2)q_d}{2x_{c0}^2} + \frac{y_{c0}}{x_{c0}}\right), \\ l_2 &= \frac{1}{2}\left(\frac{-y_{c0}q_d}{x_{c0}} + 1\right) \\ l_3 &= \frac{y_{21}}{x_{21}^2 + y_{21}^2},\ l_4 = \frac{x_{21}}{x_{21}^2 + y_{21}^2}, \\ l_5 &= -\frac{y_{c0}}{y_{c0}^2 + x_{c0}^2},\ l_6 = -\frac{x_{c0}}{y_{c0}^2 + x_{c0}^2} \end{aligned} \tag{14}$$

and

$$F = \begin{bmatrix} \frac{f(Y+B)}{m_1^2} & -\frac{f(X+D)}{m_1^2} & \frac{(X+D)^2+(Y+B)^2}{m_1^2} \\ -\frac{fh\cos\theta}{m_1^2} & -\frac{fh\sin\theta}{m_1^2} & -\frac{fhm_3}{m_1^2} \\ \frac{f(Y+B)}{m_2^2} & -\frac{f(X+D)}{m_2^2} & \frac{(X+D)^2+(Y-B)^2}{m_1^2} \\ -\frac{fh\cos\theta}{m_2^2} & -\frac{fh\sin\theta}{m_2^2} & -\frac{fhm_4}{m_2^2} \end{bmatrix}, \tag{15}$$

where m_i $(i = 1, \ldots, 4)$ are defined in (6). This representation of F is not useful because the elements are expressed in terms of the Cartesian coordinates X, Y, θ. However, it is interesting to note that multiplication of F and G gives

$$FG = \begin{bmatrix} \frac{-x_1y_1}{fh} & \frac{f^2+x_1^2}{f} \\ \frac{-y_1^2}{fh} & \frac{x_1y_1}{f} \\ \frac{-x_2y_2}{fh} & \frac{f^2+x_2^2}{f} \\ \frac{-y_2^2}{fh} & \frac{x_2y_2}{f} \end{bmatrix}. \tag{16}$$

Since J and FG have representations in terms of image coordinates x_1, y_1, x_2, y_2, image-based visual servo controller can be implemented by these matrices.

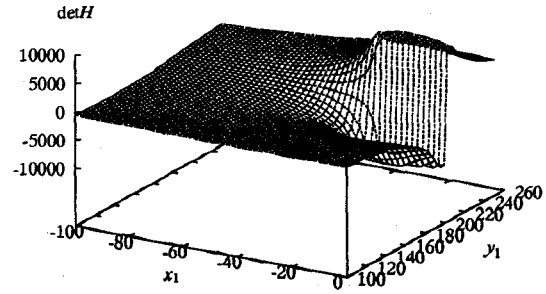

Fig. 3. Plot of det$H$ as a Function of (x_1, y_1)

VI. Control

If both the matrix $H = JFG$ and the mapping g are not singular, an exact feedback linearizing controller

$$u = -g^{-1}(H^{-1}K)z \tag{17}$$

yields the closed loop dynamics $\dot{z} = -Kz$ that makes z exponentially stable. However, H is not invertible at the reference position. To check the singularity of H in the neighborhood of ξ_d, det$H$ is plotted as a function of (x_1, y_1) for the second feature point fixed at $(X_{2d}, y_{2d}) = (f\frac{B}{D}, f\frac{h}{D})$. Figure 3 is the plot with $f = 200$ [pixel/m], $B = 0.1$ [m], $D = 1$ [m] and $h = 1$ [m].

The figure shows that the singular region exists at $y_1 = 200$ $(= f\frac{h}{D})$. Also, it can be observed that the magnitude of the determinant tends to infinity when (x_1, y_1) approaches to $(-f\frac{B}{D}, f\frac{h}{D})$. Therefore, the gain of controller (17) becomes very small when the midpoint of the features approaches to the goal point. If the orientation error exist, i.e., if $q \neq 0$, this situation is not desirable. Therefore we adopt the following *switchback* strategy:

1. Set $(x_0, y_0) = (0, \frac{fh}{D})$.
2. Observe the image.
3. If the midpoint of the current features is close to the goal point (x_0, y_0) and if the orientation q is not close to zero, then switch the reference point to a sub-goal $(x_0', y_0') = (-2fq, \frac{fh}{2D})$, otherwise continue.
4. If the midpoint of the current features is close to the switched sub-goal point (x_0', y_0'), then reset the reference point to $(x_0, y_0) = (0, \frac{fh}{D})$.
5. For a very small number ϵ, if $v > \epsilon$ then compute $u = [v\ \phi]^T$ based on (17). Otherwise, set $\phi = 0$ and compute v by (17).
6. Drive the cart. Go to 2.

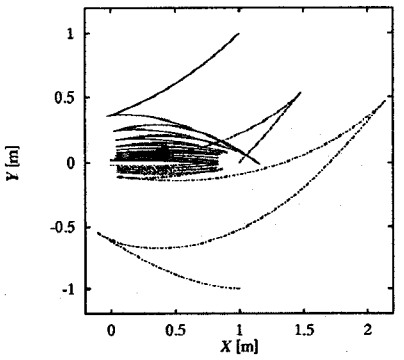

Fig. 4. Cart Motion in Cartesian Space
—: p_1, - -: p_2, - · -: p_3

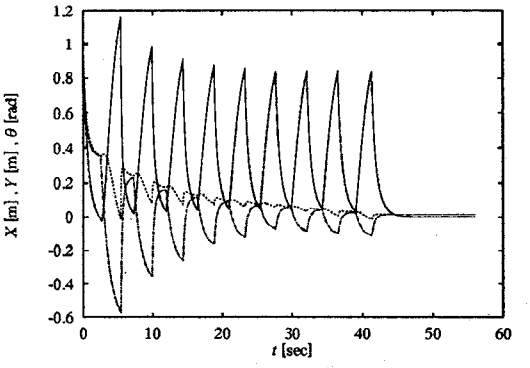

Fig. 5. Time Response in Cartesian Space (p_1)
—: X, - -: Y, - · -: θ

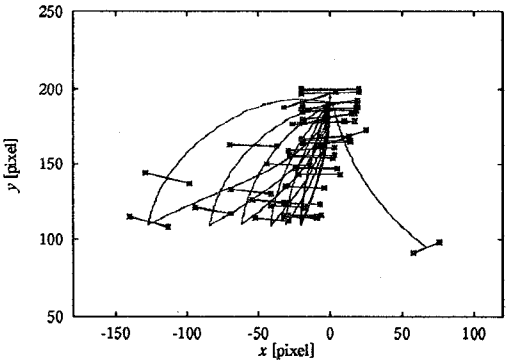

Fig. 6. Feature Trajectory in Image Space (p_1)

The second reference point $(-2fq, \frac{fh}{2D})$ used in step 3 can be modified to any point in the image plane (inside the view area) which produces switchback, i.e., almost any point $y_0 < \frac{fh}{D}$. This procedure yields switchback if the center of features approaches to the singular region with orientation error. Since the control law tries to attract the current features to the reference point along a circle connecting them, the possibility of missing feature points reduces considerably.

VII. Simulation

A. Image-based Scheme

Simulations are carried out for three initial positions, namely $p_1 = (1, 1, \pi/4)$, $p_2 = (1, 0, \pi/4)$ and $p_3 = (1, -1, 0)$. The goal position is $(0, 0, 0)$. The parameters used in this simulation are the same as that of Section VI. The sampling period is 33 [ms], which is the sampling period of the standard camera. The feature positions computed by equation (6) are rounded to the nearest integers. Switchbacks are issued if the center of the current features falls inside of a box around the desired position ($|x_c - x_0| < 10$ [pixel], $|y_c - y_0| < 10$ [pixel]) with the orientation error $|q| > 0.5$ [rad]. The simulated trajectories for three initial positions are plotted in Figure 4.

For the first initial position p_1, 9 switchbacks are generated. The time response in Cartesian space is plotted in Figure 5. The final position and orientation are $(0.00068, 0.0163, 0.0163)$. The trajectories of feature points in image plane are shown in Figure 6. The dotted line shows the trajectory of the midpoint. For every 40 samples the feature points are plotted by *s and are connected by a solid line segment to show the correspondence. The final positions of the features in the image plane are $(-20, 200, 20, 200)$. Thus, the error in Cartesian space is due to the quantization error.

For the initial position p_2, the cart initially moves backward, and then approaches to the goal followed by one switchback. It takes 10 seconds to converge to the goal position. The final position and orientation of the cart are $(0.000344, 0.0195, 0.0196)$. Figure 7 shows the trajectory of the features in the image plane. Note that the first backward motion is not due to the reference switch in Step 2 but due to the motion along a circular path in the image plane. The final error in image plane is $(0, 0, 0, 0)$.

For the initial position p_3, the cart makes one big switching and five small switchings. It takes 30 seconds to reach the goal. The final position and orientation are $(0.000197, -0.0204, 0.0204)$. The trajectory of the features in the image plane is shown in Figure 8. Though the features go close to the edge of the image plane due to the big switching, it remains inside of the image.

B. Position-based Scheme

To compare the image-based and position-based control schemes, a simulation of the controller proposed in [1] is carried out with the initial position p_3. The same gains as [1] are used. The trajectory of the cart in the Cartesian coordinates is shown in Figure 9. The trajec-

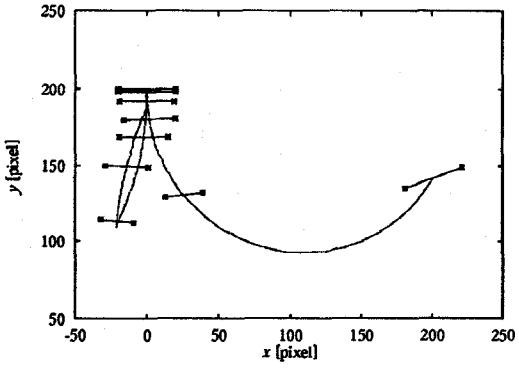

Fig. 7. Feature Trajectory in Image Space (p_2)

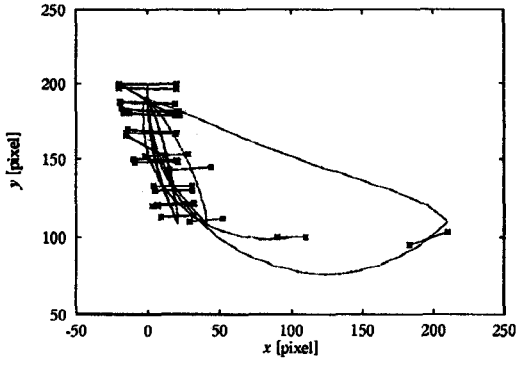

Fig. 8. Feature Trajectory in Image Space (p_3)

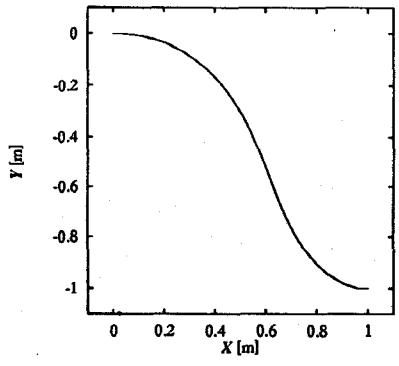

Fig. 9. Trajectory in Cartesian Space (Position-based)
—: X, - -: Y, - · -: θ

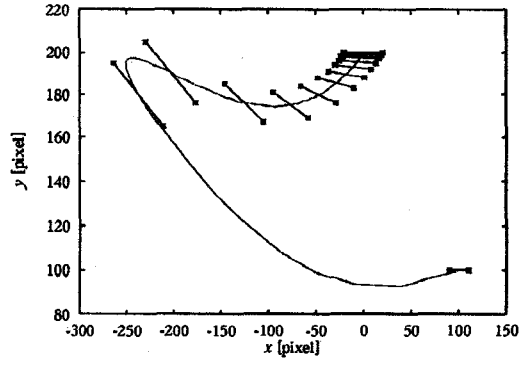

Fig. 10. Feature Trajectory in Image Space (Position-based)

tories of the features are plotted in Figure 10. Though the cart is controlled very smoothly without switchbacks, the left feature go outside of the view area.

VIII. Experiments

Experiments on a radio controlled car with a CCD camera are carried out. The wheel base is 255 [mm] and the treads are 150 [mm] for front and rear wheels. The CCD has 256 × 240 [pixel^2] and the sampling rate is 30 [Hertz]. The parameters are as follows: $f = 600, B = 0.1, D = 1, h = 0.15$. Thus the reference features are $\xi_d = (-60, 90, 60, 90)$. Figure 11 depicts the experimental setup. Since the position of mark center can be computed at sub-pixel level, the image quantization error is not very significant. However, motor control loop of the plastic model car is incomplete and have large hysteresis. Thus, it is a quite challenging problem to control the car velocity. Also we are not able to measure the cart position in the world coordinate system. Thus only the results of feature position in the image coordinates and the cart position estimated from the feature positions are shown.

An experimental result with the initial position

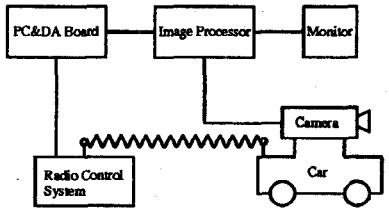

Fig. 11. Experimental Setup

$(1, 0, 0.1)$ is shown in Figures 12 and 13. The horizontal axis of Figure 12 is the time. The cart goes backward at first and approaches to the goal. The final feature position is $(-61.1, 88.9, 56.2, 88.6)$. The final cart position is $(0.014, 0.010, 0.015)$.

Another experiment is for the initial position $(1, 0.45, 0.2)$. The results are shown in Figures 14 and 15. One switchback is generated. The final feature and cart positions are $(-58.4, 89.5, 60.0, 88.0)$ and $(0.010, 0.087, 0.083)$. The cart position has small error. To eliminate this error one should use wide angle camera that makes the Jacobian F more sensitive.

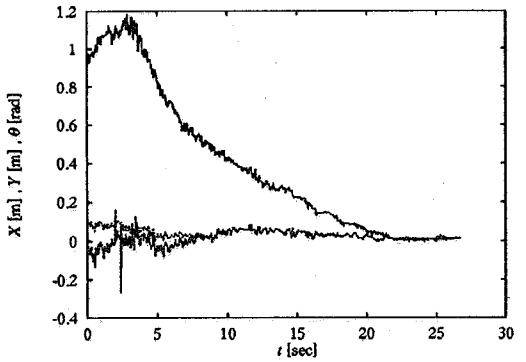

Fig. 12. Cart Trajectory in Cartesian Space

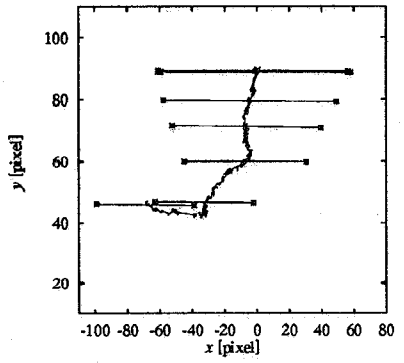

Fig. 13. Feature Trajectory in Image Space

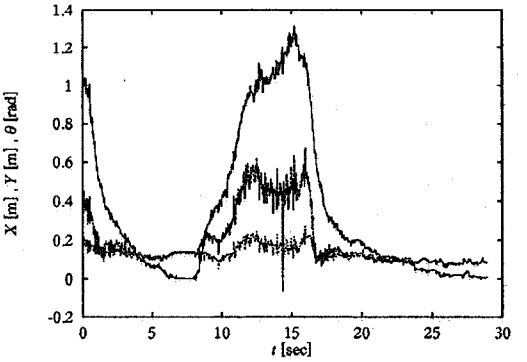

Fig. 14. Cart Trajectory in Cartesian Space

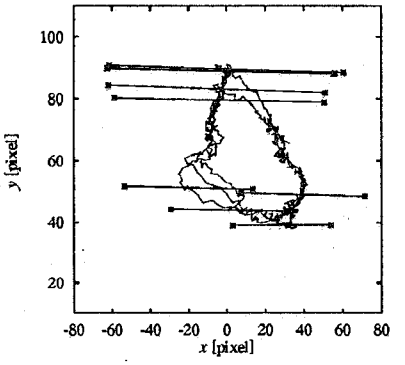

Fig. 15. Feature Trajectory in Image Space

IX. Conclusion

This paper has presented a control scheme for guiding a nonholonomic mobile robot by using visual feedback. The robot does not have capabilities for dead reckoning and a vision sensor is used to estimate the position and orientation of the robot. the nonlinear controller generates piecewise continuous command which linearizes the robot dynamics with exponential stability. Simulations and experiments have been carried out to evaluate the validity of the proposed scheme. A comparison with the position-based scheme was also made. It shows superiority of the image-based scheme in terms of the controllability of the features in the image plane.

References

[1] C. Caundas de Wit and O. J. Sørdalen, "Exponential stabilization of mobile robots with nonholonomic constraints," *IEEE Trans. Automatic Control*, vol. 37, no. 11, pp. 1791–1797, 1992.

[2] G. Lafferriere and H. Sussmann, "Motion planning for controllable systems without drift," in *IEEE Int. Conf. Robotics and Automation*, Sacramento, Calif., 1991, pp. 1148–1153.

[3] R. M. Murray and S. S. Sastry, "Nonholonomic motion planning: Steering using sinusoids," *IEEE Trans. Automatic Control*, vol. 38, no. 5, pp. 700–716, 1993.

[4] Y. Wang, "Nonholonomic motion planning: a polynomial fitting approach," in *IEEE Int. Conf. Robotics and Automation*, Minneapolis, 1996, pp. 2956–2961.

[5] B. d'Andéa Novel, G. Bastin, and G. Campion, "Modeling and control of non holonomic wheeled mobile robot," in *IEEE Int. Conf. Robotics and Automation*, Sacramento, Calif., 1991, pp. 1130–1135.

[6] C. Samson and K. Ait-Abderrahim, "Feedback control of a nonholonomic wheeled cart in Cartesian space," in *IEEE Int. Conf. Robotics and Automation*, Sacramento, Calif., 1991, pp. 1136–1141.

[7] A. Astrolfi, "Exponential stabilization of a car-like vehicle," in *IEEE Int. Conf. Robotics and Automation*, Nagoya, Japan, 1995, pp. 1391–1396.

[8] H. Khennouf and C. Canudes de Wit, "Quasi-continuous exponential stabilizers for nonholonomic systems," in *13th IFAC World Congress, Vol.F*, San Francisco, 1996, pp. 49–54.

[9] F. Bullo and R. M. Murray, "Experimental comparison of trajectory trackers for a car with trailers," in *13th IFAC World Congress, Vol.F*, San Francisco, 1996, pp. 407–412.

[10] C. Canudas de Wit, B. Siciliano, and G. Bastin eds, *Theory of Robot Control*, Springer-Verlag, Berlin, Germany, 1996.

[11] E. T. Baumgartner and S. B. Skaar, "An autonomous vision-based mobile robot," *IEEE Trans. Automatic Control*, vol. 39, no. 3, pp. 493–502, 1994.

[12] K. Hashimoto ed., *Visual Servoing —Real-Time Control of Robot Manipulators Based on Visual Sensory Feedback*, World Scientific, Singapore, 1993.

[13] R. M. Murray, Z. Li, and S. S. Sastry, *Robotic Manipulation*, CRC Press, Boca Raton, Florida, 1994.